



Legacy of contaminant N sources to the NO_3^- signature in rivers: a combined isotopic ($\delta^{15}\text{N}$ - NO_3^- , $\delta^{18}\text{O}$ - NO_3^- , $\delta^{11}\text{B}$) and microbiological investigation

Cyrielle Briand, Mathieu Sebilo, Pascale Louvat, Thierry Chesnot, Véronique Vaury, Maude Schneider, Valérie Plagnes

► To cite this version:

Cyrielle Briand, Mathieu Sebilo, Pascale Louvat, Thierry Chesnot, Véronique Vaury, et al.. Legacy of contaminant N sources to the NO_3^- signature in rivers: a combined isotopic ($\delta^{15}\text{N}$ - NO_3^- , $\delta^{18}\text{O}$ - NO_3^- , $\delta^{11}\text{B}$) and microbiological investigation. Scientific Reports, 2017, 7, pp.41703. 10.1038/srep41703 . hal-01483941

HAL Id: hal-01483941

<https://hal.sorbonne-universite.fr/hal-01483941>

Submitted on 6 Mar 2017

HAL is a multi-disciplinary open access archive for the deposit and dissemination of scientific research documents, whether they are published or not. The documents may come from teaching and research institutions in France or abroad, or from public or private research centers.

L'archive ouverte pluridisciplinaire **HAL**, est destinée au dépôt et à la diffusion de documents scientifiques de niveau recherche, publiés ou non, émanant des établissements d'enseignement et de recherche français ou étrangers, des laboratoires publics ou privés.



Distributed under a Creative Commons Attribution 4.0 International License

SCIENTIFIC REPORTS

OPEN

Legacy of contaminant N sources to the NO_3^- signature in rivers: a combined isotopic ($\delta^{15}\text{N}-\text{NO}_3^-$, $\delta^{18}\text{O}-\text{NO}_3^-$, $\delta^{11}\text{B}$) and microbiological investigation

Received: 03 August 2016
Accepted: 21 December 2016
Published: 02 February 2017

Cyrielle Briand¹, Mathieu Sebilo¹, Pascale Louvat², Thierry Chesnot³, Véronique Vaury¹, Maude Schneider³ & Valérie Plagnes⁴

Nitrate content of surface waters results from complex mixing of multiple sources, whose signatures can be modified through N reactions occurring within the different compartments of the whole catchment. Despite this complexity, the determination of nitrate origin is the first and crucial step for water resource preservation. Here, for the first time, we combined at the catchment scale stable isotopic tracers ($\delta^{15}\text{N}$ and $\delta^{18}\text{O}$ of nitrate and $\delta^{11}\text{B}$) and fecal indicators to trace nitrate sources and pathways to the stream. We tested this approach on two rivers in an agricultural region of SW France. Boron isotopic ratios evidenced inflow from anthropogenic waters, microbiological markers revealed organic contaminations from both human and animal wastes. Nitrate $\delta^{15}\text{N}$ and $\delta^{18}\text{O}$ traced inputs from the surface leaching during high flow events and from the subsurface drainage in base flow regime. They also showed that denitrification occurred within the soils before reaching the rivers. Furthermore, this study highlighted the determinant role of the soil compartment in nitrate formation and recycling with important spatial heterogeneity and temporal variability.

High nitrate concentrations in surface and ground waters remain a worldwide concern because of sanitary problems in drinking water and of ecological disturbances in aquatic systems such as eutrophication^{1–3}. Hence, the determination of nitrate origin is the first step for effective management plans aiming at preserving surface water quality. Nitrate concentrations in rivers are controlled by spatial and temporal variability of the different nitrate sources and biogeochemical or physical reactions occurring from uplands to streams^{4–6} (Fig. 1). The nitrogen and oxygen isotope ratios of NO_3^- ($\delta^{15}\text{N}$ and $\delta^{18}\text{O}$) have been widely used to investigate the sources of NO_3^- in rivers and groundwater^{4,6–14}. Actually, at the catchment scale, some N sources, such as domestic and animal effluents, present overlapping $\delta^{15}\text{N}$ ranges. The isotopic signature of nitrate results also from processes within the soils that modify its concentration (nitrification, denitrification, Fig. 1)^{15–17} fractionate its isotopes, and can blur the initial signature of the N sources. These limits can be over passed by using complementary tracers.

Previous studies have investigated boron isotope ratio ($\delta^{11}\text{B}$) to better segregate among the different nitrate sources^{18–23}. In most of the NO_3^- contamination sources, B is also substantially enriched¹⁸ and presents the advantage of not being affected by oxidation/reduction and biological reactions involving N compounds. $\delta^{11}\text{B}$ has been particularly effective at distinguishing domestic from animal effluents^{18–23}. However, B adsorption on solid surfaces such as soil particles significantly fractionates its isotopes, possibly limiting its use as tracer of sources^{18,24–27}.

In parallel, researchers have developed microbiological markers able to distinguish animal and human fecal contaminations^{28–30}. F-specific RNA phages (FRNAPHs) are viruses infecting *Escherichia Coli* and can be divided

¹UPMC Univ Paris 06, UMR IEES, 4 place Jussieu, 75252 Paris Cedex 05, France. ²Institut de Physique du Globe de Paris, Sorbonne Paris Cité, Université Paris-Diderot, UMR CNRS 7154, 1 rue Jussieu, 75238 Paris Cedex, France.

³Eurofins Expertises Environnementales, Microbiologie, Santé-Environnement, rue Lucien Cuenot/site St Jacques II, 54521 Maxeville, France. ⁴UPMC Univ Paris 06, UMR METIS, 4 place Jussieu, 75252 Paris Cedex 05, France. Correspondence and requests for materials should be addressed to C.B. (email: briandcyrielle@gmail.com)

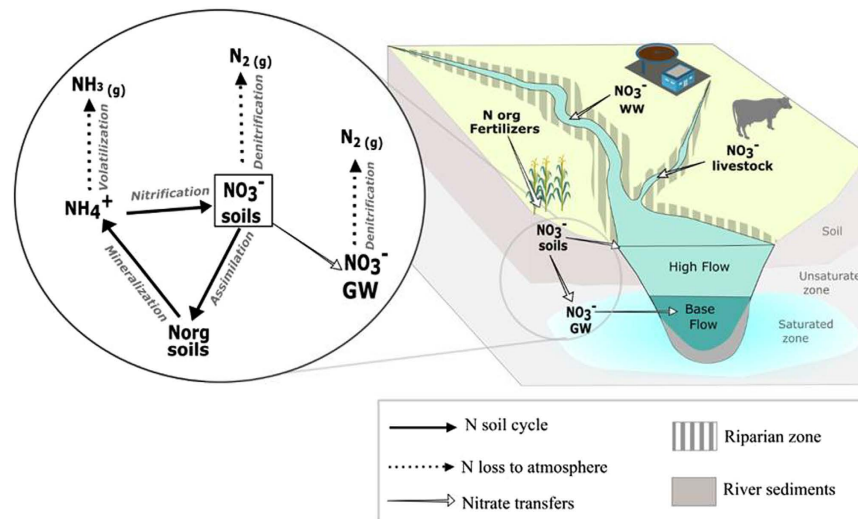


Figure 1. Schematic river catchment and its sources of nitrogen. WW = waste waters, GW = groundwater. (Created with Inkscape, version 2, <https://inkscape.org/fr/>, images from Courtesy of the Integration and Application Network, University of Maryland Center for Environmental Science (ian.umces.edu/symbols/)).

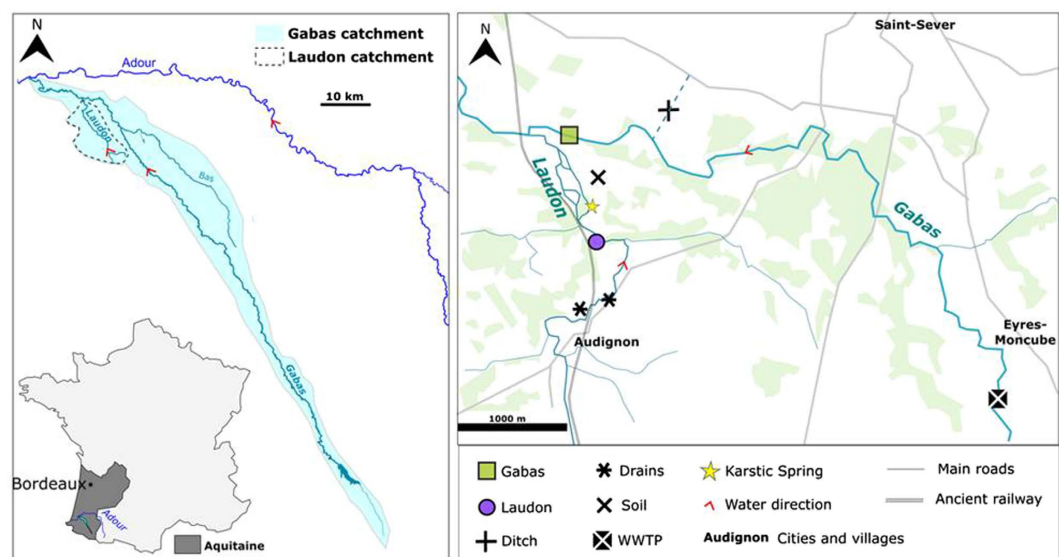


Figure 2. Left: Location of the Gabas and Laudon catchments in the southwest of France. Right: Zoom of the study area with the location of sampling points. (Created with Inkscape, version 2, <https://inkscape.org/fr/>).

into four groups (G), with GI and GIV mostly associated with animal feces and GII and GIII generally characteristic of human contamination^{31–33}. Bacteroidales are fecal bacteria with DNA sequences specific to human, cattle, pig effluents^{34–37}. These host-specificity markers have rarely been applied in natural aqueous environments^{38,39}, but their recent combination with $\delta^{15}\text{N}$, $\delta^{18}\text{O}$ and $\delta^{11}\text{B}$ has shown a great potential for determining NO_3^- origin in groundwater (GW)³⁸.

The objective of the present study was to determine the origin of nitrate in rivers where multiple nitrogen sources co-exist (Fig. 1). To do so, isotopic ($\delta^{15}\text{N}$, $\delta^{18}\text{O}$ and $\delta^{11}\text{B}$) and microbiological markers were combined for the first time at the watershed scale. This multi tracers approach was tested on two rivers of the southwest of France in an agricultural region (Fig. 2). Nitrate concentrations of Gabas River (GR, 150 km long) and Laudon River (LR, 15 km long) are a serious threat for the underlying karstic aquifer, used for drinking water supply³⁸. To better integrate the spatial heterogeneity of N point and non-point sources of the whole watershed, a 2.5 years monitoring has been conducted in the karstified downstream part of the Gabas and Laudon catchments (Fig. 2). Water sampling was carried out every two months in base flow conditions but also during flood events (Fig. 3) to characterize NO_3^- dynamics in rivers. Additionally, samples of rain, waste water treatment plant (WWTP) effluents, manure and animal fresh dejections were collected to determine the isotopic and microbiological signature

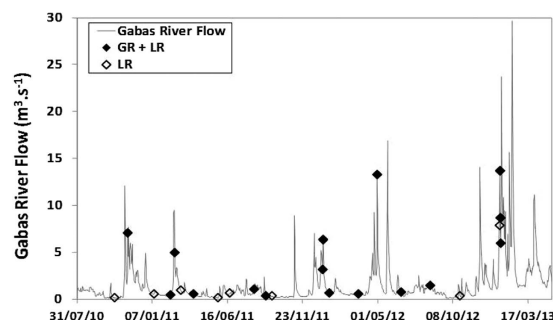


Figure 3. Timing of sampling campaigns on Gabas River and Laudon River versus the Gabas River flow rate series.

of the local N sources (Fig. 2). Finally, samples of agricultural soil, water from buried drains and surface ditch were sampled to follow the N fluxes from topsoil to rivers (Fig. 2).

Results and Discussion

Results for each tracer are first presented and discussed separately in order to understand how they can trace the different water sources but also to highlight their limits. Then we discuss how the tracer's combination allows a global understanding of NO_3^- sources, reactions and pathways.

Nitrate concentrations and stable isotopic compositions ($\delta^{18}\text{O}$ and $\delta^{15}\text{N}$): source mixing and N cycling within the soils. Nitrate concentrations $[\text{NO}_3^-]$ in Gabas River (GR) and Laudon River (LR) both ranged from 12 to 45 mg.L^{-1} (Table 1). They were globally equals to $[\text{NO}_3^-]$ of the water from surface ditch ($n = 6$) but mostly inferior to $[\text{NO}_3^-]$ of WWTP effluents ($n = 3$) and buried drains ($n = 3$) (Table 1, Fig. 4). GR and LR nitrate also exhibit similar ranges of $\delta^{15}\text{N}$ ($+8.0\text{‰}$ to $+14.6\text{‰}$) and $\delta^{18}\text{O}$ ($+3.8\text{‰}$ to $+9.3\text{‰}$, Table 1, Fig. 5) that are usually encountered for nitrate derived from organic N sources such as manure and sewage. NO_3^- extracted from topsoil samples showed the lowest $\delta^{15}\text{N}$ signatures (-11.8‰ to $+4.6\text{‰}$) with a large range of $\delta^{18}\text{O}$ ($+5.5\text{‰}$ to $+11.4\text{‰}$, Table 2, Fig. 5), whereas buried drains exhibit the highest $\delta^{15}\text{N}$ ($+11.4\text{‰}$ to $+19.6\text{‰}$) and $\delta^{18}\text{O}$ ($+7.3\text{‰}$ to $+11.0\text{‰}$, Table 1, Fig. 5).

The large gap between $\delta^{15}\text{N}$ and $\delta^{18}\text{O}$ of nitrate extracted from topsoil and nitrate of the drainage network (ditches and buried drains) reflects that important processes occur within the soils before reaching the studied rivers. *It has recently been shown that residual fraction of NO_3^- that is not immediately leached or consumed by plants is assimilated into soil organic matter and potentially recycled into NO_3^-* ⁴⁰ (Fig. 1). Some of the reactions involved in the N cycle, such as NH_4^+ volatilization and NH_4^+ nitrification are important isotope fractionating processes^{16,17,41,42}. N availability and reaction rate of each process will thus control the large $\delta^{15}\text{N}$ range of newly produced nitrate^{16,43}. Additionally, in top-soils, water evaporation and the subsequent increase of $\delta^{18}\text{O}$ - H_2O associated to root penetration will potentially lead to higher $\delta^{18}\text{O}$ - NO_3^- ⁴⁴, as 2 atoms of oxygen in NO_3^- come from the surrounding water^{7,16,45,46}. This explains why the highest $\delta^{18}\text{O}$ of soil extracted NO_3^- was measured in august 2012, under mature maize and when potential evaporation was maximum, and the lowest $\delta^{18}\text{O}$ - NO_3^- in January in absence of vegetal cover and at low temperature. Consequently, N cycling and the physical processes occurring within the soil compartment result in important temporal variations of $\delta^{15}\text{N}$ and $\delta^{18}\text{O}$ of the produced NO_3^- . These observations highlight the determinant role of the water transfer through soils over the nitrate isotopic signature, and alter the initially distinct $\delta^{15}\text{N}$ ($\delta^{15}\text{N}_{\text{urea}} = 0.9\text{‰}$, $\delta^{15}\text{N}_{\text{manure}} = 9.3\text{‰}$), and $\delta^{18}\text{O}$ (NO_3^- fertilizers vs. atmospheric deposition) of the N source end-members.

If no trend can be observed between $[\text{NO}_3^-]$ and rivers flow rates (Fig. 6), for both rivers, the lowest $\delta^{15}\text{N}$ and $\delta^{18}\text{O}$ values were mainly observed at high water stage ($>2 \text{ m}^3.\text{s}^{-1}$ for GR) whereas the highest were measured for base flow ($<2 \text{ m}^3.\text{s}^{-1}$ for GR, Fig. 6). These higher $\delta^{15}\text{N}$ values could be due to a larger contribution of an enriched pool of nitrate such as WWTP effluents ($\delta^{15}\text{N} = +10.0\text{‰}$ to $+17.3\text{‰}$) (Figs 4 and 5) during base flow compared to high flow events. However, the $\delta^{18}\text{O}$ of NO_3^- in the WWTP outlet ($+6.4\text{‰}$ to $+8.5\text{‰}$) are lower than the maximum values measured in GR and LR and thus cannot explain the $\delta^{18}\text{O}$ enrichment also observed for base flow samples (Fig. 5). Above all, considering the high $[\text{NO}_3^-]$ of WWTP effluents, a larger contribution of this of this pool should also have increased $[\text{NO}_3^-]$ in rivers, which is not observed (Fig. 4). A simple mixing of N sources thus cannot explain these high nitrate $\delta^{15}\text{N}$ and $\delta^{18}\text{O}$ during base flow and additional processes must be involved. Actually the nitrate $\delta^{15}\text{N}$ and $\delta^{18}\text{O}$ of LR samples, are pretty well distributed along the 2:1 slope expected for residual nitrate derived from denitrification^{15,16,47} (Fig. 5) and are roughly inversely correlated with $[\text{NO}_3^-]$ (Fig. 4). For the GR samples, $\delta^{15}\text{N}$ and $\delta^{18}\text{O}$ values do not strongly follow the denitrification slope but a global positive trend exists between high- and base-flow samples. Chen *et al.*⁶, reported a similar pattern with seasonal distribution in the Beijing catchment and concluded that denitrification occurred within the watershed soils, before residual NO_3^- reached the river^{6,7}.

For the samples collected under high flow conditions (Fig. 6), nitrate $\delta^{15}\text{N}$ vary largely while $\delta^{18}\text{O}$ remain quite constant, which excludes denitrification processes. In this case, the low $\delta^{15}\text{N}$ compared to base flow samples might be explained by a larger contribution of a ^{15}N depleted nitrate pool. The first possibility is that during these highly rain periods, the atmospheric nitrate ($\delta^{15}\text{N} = +1.6\text{‰}$) decreases the river $\delta^{15}\text{N}$ - NO_3^- signal. However, if such mixing process had occurred, it would also have increased the $\delta^{18}\text{O}$ - NO_3^- of rivers, which is not observed here

Sample	Date	Flow	NO ₃ ⁻	δ ¹⁵ N	δ ¹⁸ O	B	δ ¹¹ B	Bacteroidales	FRNAPHs GII
			mg.L ⁻¹	‰	‰	μg.L ⁻¹	‰	Type	>20%
Laudon	19/10/10	Base	26.2	12.7	7.7	—	—	—	—
Laudon	16/11/10	High	39.3	10.8	5.9	—	—	—	—
Laudon	11/01/11	Base	30.0	12.4	7.6	—	—	—	—
Laudon	15/02/11	Base	23.8	10.6	6.2	11.9	23.3	H C	NO
Laudon	24/02/11	High	—	—	—	—	—	H	NO
Laudon	09/03/11	Base	28.9	11.8	7.6	—	—	—	—
Laudon	05/04/11	Base	19.5	12.9	8.2	—	—	H	NO
Laudon	27/05/11	Base	20.9	12.0	7.0	—	—	—	—
Laudon	21/06/11	Base	23.6	12.7	8.2	—	—	—	—
Laudon	12/08/11	Base	26.6	12.6	8.4	1.8	13.5	—	—
Laudon	06/09/11	Base	14.3	13.4	9.3	—	—	—	—
Laudon	19/09/11	Base	15.8	12.8	8.9	13.9	25.2	C	NO
Laudon	05/01/12	High	35.1	11.4	6.4	—	—	H	NO
Laudon	06/01/12	Base	20.1	11.6	6.2	—	—	HC	YES
Laudon	19/01/12	Base	32.1	11.4	6.2	12.1	24.0	—	—
Laudon	21/03/12	Base	18.1	13.8	8.9	—	—	HC	*
Laudon	30/04/12	Base	12.0	9.8	6.2	9.2	24.2	x	—
Laudon	20/06/12	Bas	23.8	14.0	9.3	—	—	x	—
Laudon	21/08/12	Base	28.7	11.0	7.6	6.5	26.8	C	*
Laudon	23/10/12	Base	30.3	11.1	7.6	—	—	—	—
Laudon	15/01/13 16:00	High	—	—	—	—	—	H C P D	NO
Laudon	16/01/13 11:00	High	17.4	8.8	5.5	12.1	23.7	H C P D	NO
Laudon	16/01/13 16:00	High	28.2	8.0	5.4	—	—	—	—
Laudon	17/01/13 11:00	High	—	—	—	—	—	H C P D	NO
Laudon	17/01/13 15:00	High	36.3	9.1	5.6	—	—	H C P D	YES
Laudon	18/01/13	High	—	—	—	—	—	H C P D	NO
Gabas	16/11/10	High	37.2	11.6	5.9	—	—	—	—
Gabas	15/02/11	Base	20.4	12.4	9.1	7.5	21.2	C	NO
Gabas	24/02/11	High	—	—	—	—	—	H C	NO
Gabas	05/04/11	Base	18.1	13.3	7.8	—	—	H	NO
Gabas	12/08/11	Base	13.6	14.6	8.0	6.8	20.7	—	—
Gabas	06/09/11	Base	38.2	11.7	8.2	—	—	—	—
Gabas	05/01/12	High	45.4	8.6	3.8	6.1	23.5	H	YES
Gabas	06/01/12	Base	—	—	—	—	—	H C P	YES
Gabas	19/01/12	Base	34.8	11.7	7.2	—	—	—	—
Gabas	21/03/12	Base	18.2	13.5	8.4	—	—	H	YES
Gabas	30/04/12	Base	23.1	11.0	5.8	7.6	23.9	H C	*
Gabas	21/08/12	Base	19.8	12.0	7.4	4.4	26.3	H	*
Gabas	16/01/13 11:00	High	26.8	10.2	6.1	9.0	23.1	H C P D	YES
Gabas	17/01/13 11:00	High	—	—	—	—	—	H C P D	NO
Gabas	18/01/13	High	—	—	—	—	—	H C P D	YES
Ditch 1	19/01/12	Base	35.7	11.6	7.5	10.5	22.0	H	NO
Ditch 1	20/03/12	Base	20.5	11.5	7.4	13.1	17.6	H	NO
Ditch 1	30/04/12	High	18.0	10.5	5.1	10.5	18.8	H	YES
Ditch 1	17/01/13	High	40.1	9.7	7.0	10.9	17.1	H	YES
Drain 1	19/01/12	Base	56.9	19.6	11.0	7.3	26.7	—	—
Drain 2	19/01/12	Base	39.3	12.9	7.9	50.3	16.1	—	—
Drain 2	15/01/13	High	63.4	11.4	7.3	37.0	11.5	—	—
WWTP 1 effluent	19/01/12	Base	86.4	17.3	8.5	83.3	1.9	H	NO
WWTP 1 effluent	15/01/13	High	58.0	10.0	6.4	—	—	—	—
WWTP 2 effluent	19/01/12	Base	28.2	12.6	7.9	—	—	—	—
Rain	20/03/12	Base	2.7	1.6	78.6	1.6	27.7	—	—
Cretaceous Aquifer	19/10/10–17/01/13	—	23.3 ± 1.5	8.2 ± 1.2	5.5 ± 0.8	9.8 ± 2.7	24.9 ± 1.5	—	—

Table 1. Hydrological level, chemical, isotopic and microbiological results on Gabas River, Laudon River, surface ditch, buried drains, waste water treatment plant effluents (WWTP) and rain samples. Bacteroidales measured at significant concentrations (>10⁴ copies/100 mL) with H: human, C: cattle, P: pig, D: duck and FRNAPHs of GII, YES: representing more than 20% of total phages on more than 12 phages (number of plaque forming units available for typing by Petri dish), NO: GII detected <20% or <12 phages, x: under significant limit, * under quantifying limit.

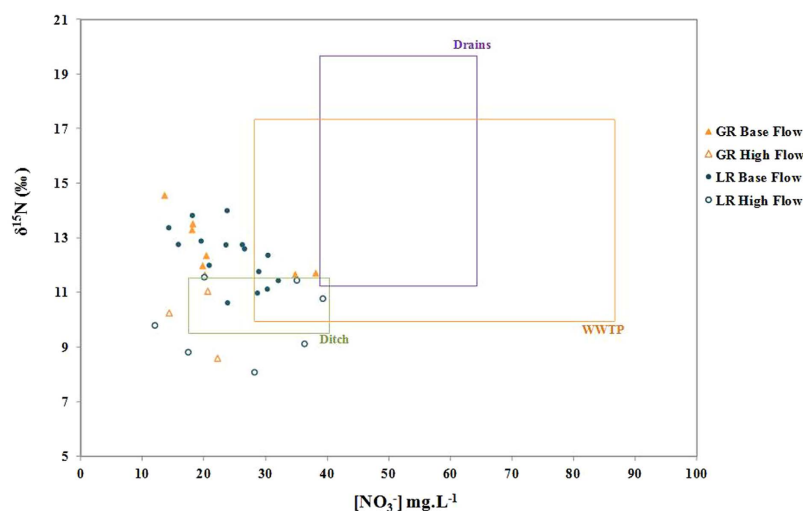


Figure 4. $\delta^{15}\text{N}$ versus nitrate concentrations measured in the Gabas River (GR) and the Laudon River (LR) during base flow and high flow regimes. Ranges measured in surface ditch, buried drains, soil extractions and wastewater plants (WWTP) effluents are reported.

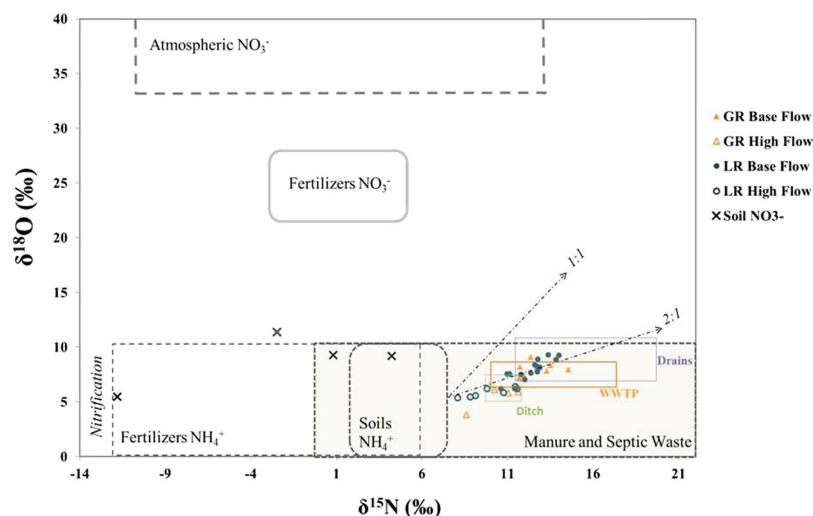


Figure 5. $\delta^{18}\text{O}$ and $\delta^{15}\text{N}$ of nitrate measured in Gabas River (GR), Laudon River (LR) during base flow and high flow. Ranges measured in surface ditch, buried drains, soil extractions and wastewater plants (WWTP) effluents are presented as well as the typical ranges of the different nitrate end-members¹⁶ and the two typical trends (1:1 and 2:1) observed in literature for denitrification.

(Fig. 6). But above all, the very low $[\text{NO}_3^-]$ of rain (2.7 mg.L^{-1} , Table 1) compared to rivers $[\text{NO}_3^-]$ during flood events (globally superior to 20 mg.L^{-1} , Table 1) seems unlikely to have impacted the global $\delta^{15}\text{N}-\text{NO}_3^-$ of rivers. The second possibility is that runoff over saturated soils brings topsoil NO_3^- , characterized by low $\delta^{15}\text{N}$ (-11.8 to $+4.2\text{‰}$), to rivers and globally decreases the river $\delta^{15}\text{N}-\text{NO}_3^-$.

Boron $\delta^{11}\text{B}$ ratios: natural versus anthropogenic signatures. Boron analyses have been carried out on GR and LR samples on the base of nitrate results, to best represent the largest variability of $[\text{NO}_3^-]$, $\delta^{15}\text{N}$ and $\delta^{18}\text{O}$. GR, LR and drainage waters, except two drain samples, were characterized by low boron concentrations (1.8 to $14.9 \mu\text{g.L}^{-1}$, Table 1, Fig. 7), usually encountered in uncontaminated water^{19,48}. The $\delta^{11}\text{B}$ of these samples ($+13.5\text{‰}$ and $+26.8\text{‰}$) plots into the overlapping typical ranges of rain⁴⁰ and manure sources^{19,42} (Fig. 7). The $\delta^{11}\text{B}$ measured for local rain (27.7‰) and WWTP effluents (1.9‰) were in good agreement with the ranges reported in literature for atmospheric and domestic boron^{19,22} (Fig. 7). However, the characterization of local animal pool (fresh dejection $\delta^{11}\text{B} = -3.3\text{‰}$ and poultry manure $\delta^{11}\text{B} = +8.6\text{‰}$) shows lower values than previously reported ($+15.3\text{‰}$ to $+27.6\text{‰}$)¹⁹. Globally, $[\text{B}]$ and $\delta^{11}\text{B}$ of the GR and LR samples were really close to those measured in the underlying karstic aquifer ($10.5 \pm 2 \text{ ppb}$ and $25.3 \pm 1\text{‰}$)³⁸, and in rain, and were significantly different from the WWTP end-member (Fig. 7).

Solid Samples	Date	NO ₃ ⁻	δ ¹⁵ N	δ ¹⁸ O	B	δ ¹¹ B
		mg.g ⁻¹	‰	‰	μg.g ⁻¹	‰
Soil Extraction	27/09/2011	52	4.2	9.2	—	—
Soil Extraction	14/12/2011	17	0.8	9.3	—	—
Soil Extraction	24/08/2012	23	-2.5	11.4	—	—
Soil Extraction	18/01/2013	16	-11.8	5.5	—	—
Urea	—	—	0.9	—	<LD	*
Poultry Manure	—	—	9.3	—	5	8.6
Poultry Fresh Dejection	—	—	3.6	—	23	-3.3

Table 2. Chemical and isotopic data measured for soil extracted nitrates and solid samples of chemical fertilizers (urea), poultry fresh dejection and manure.

The isotopic shift between the measured δ¹¹B values and those usually referenced for the animal pool may be due to the different experimental procedures: total digestion by alkaline fuse for our measurements versus leaching for the literature values. The ¹⁰B has a greater affinity for sorption onto solid surfaces^{24,25,27} than ¹¹B, and leaching experiments might have induced an isotopic fractionation towards higher δ¹¹B in the leach solutions compared to the bulk values from alkaline fusion. The measured δ¹¹B signatures of the animal end-member plot close to the domestic (WWTP) pool, making δ¹¹B not effective to distinguish animal from human contamination. Drain 2 exhibits higher [B] and lower δ¹¹B than the other surface water samples and could reflect a more important contribution of animal or domestic contamination.

Microbiological markers: animal versus domestic contamination. Human *Bacteroidales* were encountered at significant concentrations (>10⁴ copies/100 mL) in WWTP effluents (n = 1), in the 4 ditch samples and in GR (10 times among 11 analyzed samples, or 10/11) and LR (11/15) under both base and high-flow rates (Table 1). This domestic fecal contamination was corroborated by the detection of FRNAPHs of Group II at significant concentrations (proportion greater than 20% of total phages counted on more than 12 phages) in two of the 4 ditch samples, in 2 high flow LR samples and in both high- (n = 3) and base-flow (n = 2) GR samples (Table 1). These results are consistent with the fact that domestic rejects are constant and do not depend on hydrology or season. Animal contamination was pointed out in both rivers. Among the eleven samples from GR, cattle and pig markers were detected in respectively 7 and 4 samples, mostly collected under high flow conditions. Among the 15 samples of LR, cattle *Bacteroidales* were detected ten times in both high (6/10) and base flow samples (4/10) while pig markers were only detected in high flow samples (5/15). Finally, duck-chicken-geese marker was tested during the flood event of the last campaign and was detected in all GR and LR samples. These results reflect that runoff is the major pathway of microorganisms from animal sources to rivers through surface leaching during rainy events, but the markers do not allow to distinguish contamination from point sources, such as fresh dejections in farms, and non-point sources, such as manure spread on fields. However, as no animal marker was found (at significant concentration) in the ditches that drain maize fields, it could traduce that animal contamination measured in GR and LR rather arises from farming rather than from manure spread on fields. For LR, the regular presence of cows in the Laudon 200m upstream the sampling point can explain how cattle markers can reach the LR in absence of rain event.

The microbiological tracers undeniably indicate that domestic and animal fecal contaminations do impact the two rivers and thus can potentially contribute to NO₃⁻ contents of GR and LR.

Processes and pathways within catchment. In this study, anthropogenic contaminations have been evidenced by δ¹¹B in the LR and GR rivers (without possible distinction between WWTP and animal sources), and both animal and human microbiological markers have been detected. Because the identified sources of microbiological tracers and of boron also contain high N levels, their combination with the δ¹⁵N and δ¹⁸O of nitrates offers a better understanding of the processes and pathways of nitrates to the rivers as the δ¹¹B signatures of the rain and GW are significantly different from those of animal and domestic sources, they can be used for tracing and quantifying the proportions of B arising from these different groups of B sources. A simple mixing calculation (details in Methods) based on δ¹¹B and [B] of three potential B sources (karstic groundwater, WWTP effluents and rainwater) was applied to each river sample. Results indicate that the atmospheric pool is the main source of boron to the rivers (50 to 96%), while groundwater brings a smaller proportion of boron (4 to 45%) and that domestic effluents (WWTP) contribute to a maximum of 10% of the total river boron (0 to 5% for GR and 0 to 10% for LR). This simplified model does not integrate the animal end-member because alkaline fusion procedure did not allow to characterize [B] arising from animal manure and fresh dejection leaching. However, considering the overlapping δ¹¹B signatures of the animal and domestic effluents, it comes that at least a part of the calculated WWTP contribution could actually be of animal origin. Alternatively, the low [B] and high δ¹¹B measured in GR and LR could also result from B adsorption onto soils particles before boron reached rivers with an isotopic ¹¹B enrichment^{20,39,50}. Such a process could have blurred a larger contribution of domestic and/or animal effluents than previously deduced through the mixing calculation. B adsorption is more prone to occur within soils and GW (longer water residence time and higher rock/water ratio) than during surface leaching or within the rivers, and it is already expressed in the δ¹¹B signatures of the GW and drainage samples (drains and ditches). The similar B signatures of GW and rain can explain the high constancy of [B] and δ¹¹B measured in the two rivers during base flow, when GW is the major water source, as well as during high flow episodes, when rain

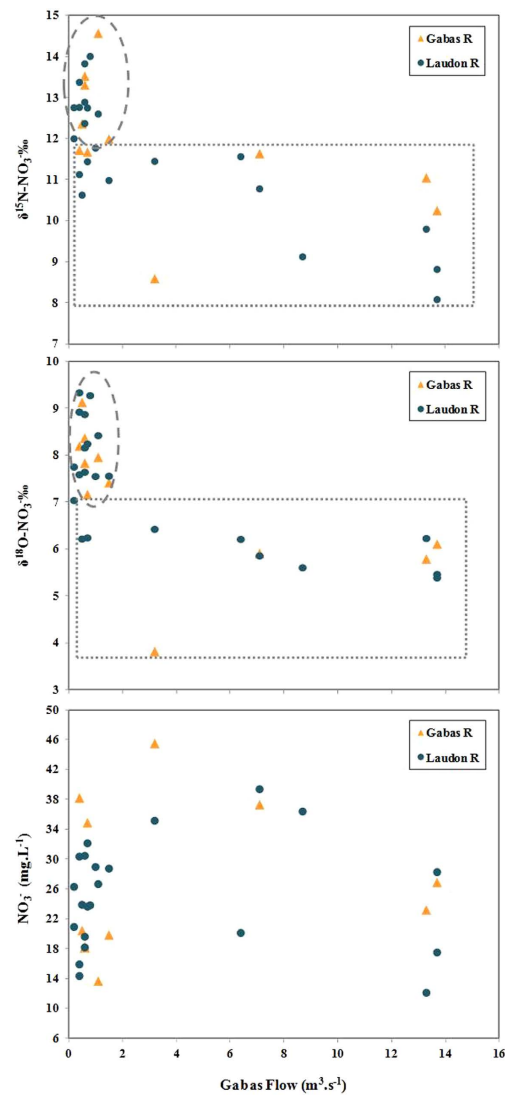


Figure 6. Nitrate concentrations, $\delta^{15}\text{N}$ and $\delta^{18}\text{O}$ depending on the Gabas River flow ($\text{m}^3.\text{s}^{-1}$) measured in the middle part of the Gabas section.

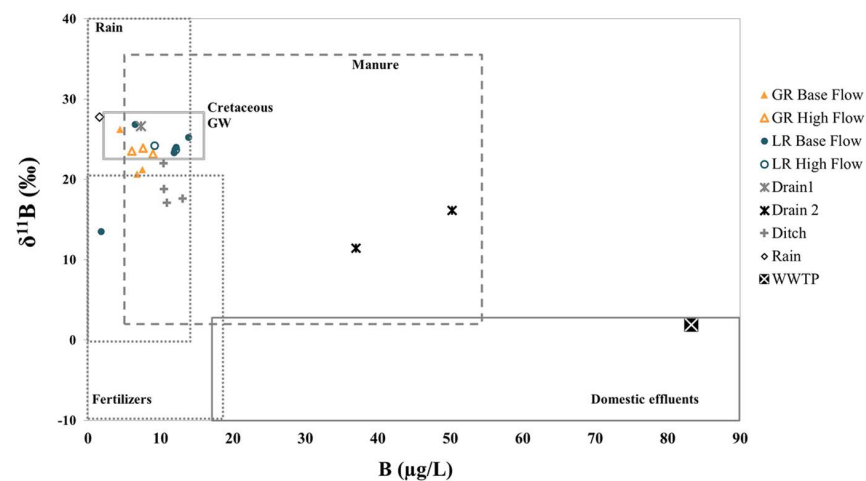


Figure 7. $\delta^{11}\text{B}$ versus concentration of boron in surface water (Gabas River, Laudon River, drains, ditch), WWTP effluents and rain. Expected ranges reported in literature for boron end members are also presented^{19,38,48–50}.

contribution strongly increases. If microbiological tracers have shown that domestic and WWTP effluents are permanent contaminations for GR and LR, the denitrification signal identified by $\delta^{15}\text{N}$ and $\delta^{18}\text{O}$ of the GR and LR nitrates for base flow samples only associated with constant $\delta^{11}\text{B}$ should rather reflect changes of NO_3^- pathways than changes of NO_3^- sources. During base flow regime, soils are not saturated, rain or irrigation water infiltrate within the soils carrying dissolved nitrate to the saturated zone where chemical and physical conditions (temperature, soil humidity, dissolved oxygen concentrations...) and agricultural practices (N-fertilizer input periods) control the degree of denitrification. In absence of surface runoff, this shallow GW is the major source of water to GR and LR, bringing denitrified nitrate to rivers. This hypothesis is comforted by the high $[\text{NO}_3^-]$, $\delta^{15}\text{N}$ and $\delta^{18}\text{O}$ measured in the buried drains (Figs 4 and 5) but also by the close boron signatures of drain 1, LR and GR samples. On the contrary, when the soils of the catchment are saturated, runoff increases river's flows and surface leaching. Topsoil nitrates, that have not yet undergone denitrification, thus become an additional NO_3^- source for rivers. These nitrates arise, at least partially, from animal sources, as was deduced from the detection of cattle microbiological markers.

Conclusion

Isotopic and microbiological tracers have proven very powerful for the determination and characterization of contaminant sources to rivers. However, physical and chemical reactions of the N cycle within the soils blur the initial N signatures and soils become an additional source of newly produced (or transformed) nitrate, which contribution to the river depends on the hydrological stage of the catchment. That's why combining of these different tracers associated to temporal monitoring are required to explain the variations of nitrate concentrations and isotopic signatures measured in the two rivers. In the present agricultural catchment with nitrate pollution threat to the underlying karstic aquifer, anthropogenic contaminations were identified through $\delta^{11}\text{B}$ measurements, microbiological tracers recorded animal dejections during high-flow stages but permanent human effluents. $\delta^{15}\text{N}$ and $\delta^{18}\text{O}$ of nitrate allowed to understand the N-cycle within the soils and its impact on the nitrate pathways to the rivers. It thus appears essential to monitor at least as much as for rivers themselves, the spatial heterogeneity and the temporal variability of nitrate concentrations and isotopic compositions in topsoil but also in drains and ditches in order to characterize the contribution of soil to the global nitrate content of rivers. This study also highlighted the crucial impact of hydrological conditions on nitrate contents and signature in rivers.

Methods

Study site. Located in the southwest of France, Gabas River and its tributary Laudon River, respectively drain catchment areas of 420 km² and 50 km²⁵¹ (Fig. 2). In the upstream part of its catchment, Gabas dug into sandy-clay molasses of Eo-Miocene. In the downstream part, Gabas and Laudon incise Cretaceous and Eocene karstic carbonate formations (anticline structure). Reliefs correspond to Miocene sandy formation and represent potential perched aquifers of little extension⁵¹. Gabas catchment and the sub-catchment of Laudon are mainly devoted to agriculture (80% of the total surface) with intensive maize cultivation and farms, evolving from cattle and pigs in the upstream part to poultry in the downstream part⁵¹. The two rivers are largely used for maize irrigation from April-May to August-September, depending on spring and summer rainfalls. Potential local sources of nitrate are thus, urea and manure applied on maize fields, nitrification of soil organic matter, livestock slurry and domestic effluents. The high $[\text{NO}_3^-]$ regularly measured in GR and LR, close to the European drinking limit of 50 mg $\text{NO}_3^- \cdot \text{L}^{-1}$ (European Directive 98/83/CE), represents a serious threat for the underlying karstic aquifer which is a strategic resource of drinking water⁵¹. Base flow of Gabas is around 1 to 3 m³/s (Fig. 3) and if it is globally inferior for Laudon with 0.5 m³/s, the variations of water levels are synchronous between the two streams. Flood responses are very rapid (a few hours), with maximum flows above 10 m³/s and 1 m³/s respectively for GR and LR.

Sampling strategy. Rivers water sampling has been carried out from October 2010 to January 2013. Sampling was realized at the very output of each watershed (Fig. 2) to better integrate the different point and non-point sources of nitrate occurring in the whole catchments and that potentially infiltrate to groundwater through the karstic outcrops. As agricultural activities evolve within the year whereas domestic inputs are more constant, sampling has been realized at different step of agricultural practices: before and after N inputs, under and without maize cover, in order to follow potential changes in agricultural/domestic contributions. Moreover, because biogeochemical processes affecting nitrate depend on parameters such as meteorology and hydrology, samples have been collected under different hydrological conditions: during base flow regimes and flood events (Fig. 3).

LR and GR were sampled 1 km before their confluence (Fig. 2). The lack of automatic measurements of LR flow rates forced us to use the Gabas chronicles for the interpretation of the LR data.

The different local potential sources of nitrate were collected to characterize their isotopic signature. Solid samples of fertilizers (urea pellets), cattle manure and fresh dejections (ducks) were provided by local farmers. Wastewater treatment plant effluents were sampled three times before its discharge in GR (Fig. 2). Rainwater samples have been collected in the downstream part of the GR catchment, less than 1 km from both river monitoring points (Fig. 2). An agricultural soil (maize field) located in the Laudon catchment (Fig. 2) has been sampled four times, between September 2011 and January 2013 under dry and rainy conditions and at different stages of maize growth. This type of soil is assumed to be representative of the whole Laudon's catchment and of the downstream part of Gabas catchment. Extraction of nitrate from these topsoil samples was performed to characterize their isotopic composition. To do so, soil was dried and crushed above 200 μm , 70 g of soil were added to 140 ml of 0.5M KCl. The mixture was agitated for 2 hours (250 rotations per minute or rpm), centrifuged at 8000 rpm during 35 minutes and filtrated on 0.45 μm nylon membrane. Finally, surface runoff and subsurface drainage have been collected from one ditch and two buried plastic drains (Fig. 2).

All water samples were filtered on 0.45 μm nylon membrane and dispatched into three polyethylene bottles. A fraction (60 ml) of total filtered sample was stored frozen for nitrate and other major anions concentration

measurement, another (60 ml) was poisoned with HgCl_2 (6%) for measurement of isotopic composition of nitrate and a third (250 mL) was acidified to pH = 2 with ultra-pure HNO_3 for analysis of boron concentration and isotopic ratio but also major cations concentrations. The physical and chemical parameters and concentrations of major anions and cations are available in a supplementary file (Supplementary Table S1).

Nitrate concentrations, $\delta^{15}\text{N}$ and $\delta^{18}\text{O}$. For waters and soil extracted samples, nitrate concentrations were analyzed by high-performance liquid chromatography (HPLC Dionex, AS12 column; Thermo Scientific, Sunnyvale, CA, USA). $\delta^{15}\text{N}$ and $\delta^{18}\text{O}$ of NO_3^- were determined using the chemical denitrification modified from McIlvin & Altabet⁵² on an isotope ratio mass spectrometer (IRMS, DeltaVplus; Thermo Scientific, Bremen, Germany) in continuous-flow with a purge and trap system coupled with a Finnigan GasBench II system (Thermo Scientific). First step was nitrate reduction to nitrite. Sample, prepared in a salted buffer ($\text{NaCl} = 0.5 \text{ M}$; $\text{pH} = 8.5$) at $20 \mu\text{mol NO}_3^- \cdot \text{L}^{-1}$ passed through a granular activated-cadmium column. Produced NO_2^- was then converted to N_2O by adding azide (NaN_3) in a 15 mL solution at $1 \mu\text{mol NO}_2^- \cdot \text{L}^{-1}$ sealed in a glass vial. Denitrification reaction was stopped by adding sodium hydroxide to avoid formation of N_2 ⁵³. The method was calibrated with nitrate standards (USGS-32, $\delta^{15}\text{N} = 180\text{‰}$, $\delta^{18}\text{O} = 25.7\text{‰}$; USGS-34, $\delta^{15}\text{N} = -1.8\text{‰}$, $\delta^{18}\text{O} = -27.9\text{‰}$ and USGS-35 $\delta^{15}\text{N} = 2.7\text{‰}$, $\delta^{18}\text{O} = 57.5\text{‰}$) and verified with an international standard nitrate (IAEA-NO-3, $\delta^{15}\text{N} = 4.7\text{‰}$, $\delta^{18}\text{O} = 25.6\text{‰}$). The precision for $\delta^{15}\text{N}$ was 0.8‰ and 1‰ for $\delta^{18}\text{O}$ (1SD).

Solid samples were air-dried, ground and sealed in tin capsules introduced in an elemental analyzer (Vario PYRO cube, Elementar) where they were oxidized by combustion (at 1120°C) and reduced into N_2 . $\delta^{15}\text{N}$ of N_2 was measured with coupled IRMS (IsoPrime, micromass). Calibration was realized with international standards of ammonium sulfate (IAEA-305A, $\delta^{15}\text{N} = +39.8 \pm 0.7\text{‰}$) and an intern standard (Tyrosine, $\delta^{15}\text{N} = +10.01\text{‰}$). The precision for $\delta^{15}\text{N}$ was 0.3‰ (SD).

Boron concentrations, $\delta^{11}\text{B}$ and mixing model. [B] and $\delta^{11}\text{B}$ analysis. Samples for B analysis have been selected on the base of nitrate concentrations, $\delta^{15}\text{N}$ and $\delta^{18}\text{O}$ to represent the largest variability. B concentrations were determined on an inductively coupled plasma atomic emission spectroscopy (ICP-OES/AES JY2000). The $^{11}\text{B}/^{10}\text{B}$ isotopic ratios were measured by MC-ICP-MS (Neptune, Thermo Scientific) using a direct-injection nebulizer (d-DIHEN, Analab)⁵⁴. Preliminary B extraction is performed by ion exchange chromatography on Amberlite IRA-743 anionic resin. Retained B was then eluted with HNO_3 (0.1 and 0.5N)⁵⁴. $\delta^{11}\text{B}$ were measured by sample-standard bracketing with SRM NBS-951 (NIST) boron international standard. Average repeatability of $\delta^{11}\text{B}$ measurements for triplicate analyses of natural water samples was 0.25‰ (2SD)⁵⁴.

Mixing model. For each of the Gabas and Laudon river samples (riv), we calculate the proportions (α_x) of B arising from rain (R), Cretaceous groundwater (GW) and waste-water treatment plants effluents (WWTP) from a set of three mass budget equations on $[\text{B}]_x$ and $\delta^{11}\text{B}_x$:

$$\alpha_R + \alpha_{\text{GW}} + \alpha_{\text{WWTP}} = 1 \quad (1)$$

$$[\text{B}]_{\text{riv}} = \alpha_R [\text{B}]_R + \alpha_{\text{GW}} [\text{B}]_{\text{GW}} + \alpha_{\text{WWTP}} [\text{B}]_{\text{WWTP}} \quad (2)$$

$$\delta^{11}\text{B}_{\text{riv}} = \alpha_R \delta^{11}\text{B}_R + \alpha_{\text{GW}} \delta^{11}\text{B}_{\text{GW}} + \alpha_{\text{WWTP}} \delta^{11}\text{B}_{\text{WWTP}} \quad (3)$$

The [B] and $\delta^{11}\text{B}$ values of the mixing end-members were measured in this study (rain and WWTP) or in a previous one (GW)³⁸. Rain: $[\text{B}]_R = 1.6 \pm 1 \text{ ppb}$ and $\delta^{11}\text{B}_R = 27.7 \pm 7\text{‰}$; Groundwater: $[\text{B}]_{\text{GW}} = 10.5 \pm 2 \text{ ppb}$ and $\delta^{11}\text{B}_{\text{GW}} = 25.3 \pm 1\text{‰}$; WWTP: $[\text{B}]_{\text{WWTP}} = 83.3 \pm 3 \text{ ppb}$ and $\delta^{11}\text{B}_{\text{WWTP}} = 1.9 \pm 2\text{‰}$;

As discussed in the main text, the mixing doesn't take into account a possible B input from animal dejections and manure, due to the difficulty of defining an aqueous [B] for this solid end-member. However, its $\delta^{11}\text{B}$ signature (8.6 and -3.3‰) is intermediate between WWTP and river $\delta^{11}\text{B}$. Thus, the proportion of B arising from WWTP may in fact incorporate animal B input, which cannot be calculated.

Microbiological Analyses: FRNAPHs and Bacteroidales. Microbiological samples were stored in sterile dedicated flask containing sodium thiosulphate salt (neutralizing agent effective against a wide range of oxidizing substances) used to preserve microorganism. FRNAPHs were enumerated after concentrating 1L of water sample using the membrane filtration-elution method⁵⁵. Infectious FRNAPHs were counted (double agar-layer technique), collected, re-suspended in 1 mL of PBS with 15% glycerol and stored at -20°C (standard NF EN ISO 10705-1: 2001). Genotyping was performed by one-step real time, reverse transcription polymerase chain reaction (RT-qPCR)⁵⁶. Research of *Bacteroidales* markers (HF183, Rum-2Bac, BacR, BacB2, Pig-1-Bac and Pig-2-Bac) was performed by filtering 1L of sample water through a $0.22 \mu\text{m}$ pore size polycarbonate membrane. Filter was immersed in a GITC lyses solution and stored at -80°C . DNA extraction was performed with the Qiamp DNA minikit (Qiagen). Standard curves were calculated for plasmids containing the target sequence. PCR reactions were duplicated for each sample and measurements were performed using a Rotor gene 6000 thermocycler. The results are expressed as a number of copies in 100 mL of water.

References

- Spalding, R. F. & Exner, M. E. Occurrence of Nitrate in Groundwater—A Review. *Journal of Environment Quality* **22**, 392 (1993).
- WHO|The world health report 2007 - A safer future: global public health security in the 21st century. WHO Available at: <http://www.who.int/whr/2007/en/>. (Accessed: 8th March 2016).
- WHO|The World Health Report 2008 - primary Health Care (Now More Than Ever). WHO Available at: <http://www.who.int/whr/2008/en/>. (Accessed: 8th March 2016).

4. Sebiló, M., Billen, G., Grably, M. & Mariotti, A. Isotopic composition of nitrate-nitrogen as a marker of riparian and benthic denitrification at the scale of the whole Seine River system. *Biogeochemistry* **63**, 35–51 (2003).
5. McClain, M. E. *et al.* Biogeochemical Hot Spots and Hot Moments at the Interface of Terrestrial and Aquatic Ecosystems. *Ecosystems* **6**, 301–312 (2003).
6. Chen, F., Jia, G. & Chen, J. Nitrate sources and watershed denitrification inferred from nitrate dual isotopes in the Beiji River, south China. *Biogeochemistry* **94**, 163–174 (2009).
7. Panno, S., Hackley, K., Hwang, H. & Kelly, W. Determination of the sources of nitrate contamination in karst springs using isotopic and chemical indicators. *Chemical Geology* **179**, 113–128 (2001).
8. Robinson, D. $\delta^{15}\text{N}$ as an integrator of the nitrogen cycle. *Trends in Ecology & Evolution* **16**, 153–162 (2001).
9. Burns, D. A., Boyer, E. W., Elliott, E. M. & Kendall, C. Sources and Transformations of Nitrate from Streams Draining Varying Land Uses: Evidence from Dual Isotope Analysis. *Journal of Environment Quality* **38**, 1149 (2009).
10. Xue, D. *et al.* Present limitations and future prospects of stable isotope methods for nitrate source identification in surface- and groundwater. *Water Research* **43**, 1159–1170 (2009).
11. Billy, C., Billen, G., Sebiló, M., Birgand, F. & Tournebise, J. Nitrogen isotopic composition of leached nitrate and soil organic matter as an indicator of denitrification in a sloping drained agricultural plot and adjacent uncultivated riparian buffer strips. *Soil Biology and Biochemistry* **42**, 108–117 (2010).
12. El Gaozi, F.-Z. J. *et al.* Using $\delta^{15}\text{N}$ and $\delta^{18}\text{O}$ values to identify sources of nitrate in karstic springs in the Paris basin (France). *Applied Geochemistry* **35**, 230–243 (2013).
13. Li, S.-L. *et al.* Evaluation of nitrate source in surface water of southwestern China based on stable isotopes. *Environ Earth Sci* **68**, 219–228 (2013).
14. Ding, J. *et al.* Identifying diffused nitrate sources in a stream in an agricultural field using a dual isotopic approach. *Science of The Total Environment* **484**, 10–18 (2014).
15. Böttcher, J., Strebel, O., Voerkelius, S. & Schmidt, H.-L. Using isotope fractionation of nitrate-nitrogen and nitrate-oxygen for evaluation of microbial denitrification in a sandy aquifer. *Journal of Hydrology* **114**, 413–424 (1990).
16. Kendall, C. & McDonnell, J. J. In *Isotopes tracers in Catchment Hydrology* 519–576 (1998).
17. Kendall, C., Elliott, E. M. & Wankel, Scott D. In *Stable isotopes in Ecology and Environmental Science* 375–449 (Blackwell Publishing, 2007).
18. Leenhouts, J. M., Basset, R. I. & Iii, T. M. Utilization of Intrinsic Boron Isotopes as Co-Migrating Tracers for Identifying Potential Nitrate Contamination Sources. *Ground Water* **36**, 240–250 (1998).
19. David Widory, W. K. Nitrate in groundwater: an isotopic multi-tracer approach. *Journal of contaminant hydrology* **72**, 165–88 (2004).
20. Seiler, R. L. Combined use of ^{15}N and ^{18}O of nitrate and ^{11}B to evaluate nitrate contamination in groundwater. *Applied Geochemistry* **20**, 1626–1636 (2005).
21. Widory, D., Petelet-Giraud, E., Négrel, P. & Ladouche, B. Tracking the Sources of Nitrate in Groundwater Using Coupled Nitrogen and Boron Isotopes: A Synthesis. *Environ. Sci. Technol.* **39**, 539–548 (2005).
22. Bronders, J. *et al.* Use of Compound-Specific Nitrogen (d^{15}N), Oxygen (d^{18}O), and Bulk Boron (d^{11}B) Isotope Ratios to Identify Sources of Nitrate-Contaminated Waters: A Guideline to Identify Polluters. *Environmental Forensics* **13**, 32–38 (2012).
23. Widory, D. *et al.* Improving the management of nitrate pollution in water by the use of isotope monitoring: the $\delta^{15}\text{N}$, $\delta^{18}\text{O}$ and $\delta^{11}\text{B}$ triptych. *Isotopes Environ Health Stud* **49**, 29–47 (2013).
24. Keren, R., Gast, R. G. & Bar-Yosef, B. pH-Dependent Boron Adsorption by Na-Montmorillonite. *Soil Science Society of America Journal* **45**, 45 (1981).
25. Palmer, M. R., Spivack, A. J. & Edmond, J. M. Temperature and pH controls over isotopic fractionation during adsorption of boron on marine clay. *Geochimica et Cosmochimica Acta* **51**, 2319–2323 (1987).
26. Barth, S. R. Boron Isotopic Compositions of Near-Surface Fluids: A Tracer for Identification of Natural and Anthropogenic Contaminant Sources. *Water, Air, & Soil Pollution* **124**, 49–60 (2000).
27. Goldberg, S., Lesch, S. M. & Suarez, D. L. Predicting Boron Adsorption by Soils Using Soil Chemical Parameters in the Constant Capacitance Model. *Soil Science Society of America Journal* **64**, 1356 (2000).
28. Blanch, A. R. *et al.* Integrated Analysis of Established and Novel Microbial and Chemical Methods for Microbial Source Tracking. *Appl. Environ. Microbiol.* **72**, 5915–5926 (2006).
29. Gourmelon, M. *et al.* Development of microbial and chemical MST tools to identify the origin of the faecal pollution in bathing and shellfish harvesting waters in France. *Water Research* **44**, 4812–4824 (2010).
30. Pourcher, A. M. *et al.* Des micro-organismes et des composés chimiques pour identifier les sources de contamination fécale: étude de leur persistance en microcosmes et de leur présence dans les eaux à l'échelle d'un bassin versant. *Sciences Eaux and Territoires : la Revue du IRSTEA* 92–97 (2012).
31. Hsu, F. C., Shieh, Y. S., Duin, J. van, Beekwilder, M. J. & Sobsey, M. D. Genotyping male-specific RNA coliphages by hybridization with oligonucleotide probes. *Appl. Environ. Microbiol.* **61**, 3960–3966 (1995).
32. Schaper, M., Jofre, J., Uys, M. & Grabow, W. o. k. Distribution of genotypes of F-specific RNA bacteriophages in human and non-human sources of faecal pollution in South Africa and Spain. *Journal of Applied Microbiology* **92**, 657–667 (2002).
33. Ogorzal, L. & Gantzer, C. Development of real-time RT-PCR methods for specific detection of F-specific RNA bacteriophage genogroups: Application to urban raw wastewater. *Journal of Virological Methods* **138**, 131–139 (2006).
34. Seurinck, S., Defoirdt, T., Verstraete, W. & Siciliano, S. D. Detection and quantification of the human-specific HF183 Bacteroides 16S rRNA genetic marker with real-time PCR for assessment of human faecal pollution in freshwater. *Environmental Microbiology* **7**, 249–259 (2005).
35. Layton, A. *et al.* Development of Bacteroides 16S rRNA Gene TaqMan-Based Real-Time PCR Assays for Estimation of Total, Human, and Bovine Faecal Pollution in Water. *Appl. Environ. Microbiol.* **72**, 4214–4224 (2006).
36. Mieszkina, S., Furet, J.-P., Corthier, G. & Gourmelon, M. Estimation of Pig Faecal Contamination in a River Catchment by Real-Time PCR Using Two Pig-Specific Bacteroidales 16S rRNA Genetic Markers. *Appl. Environ. Microbiol.* **75**, 3045–3054 (2009).
37. Mieszkina, S., Yala, J.-F., Joubrel, R. & Gourmelon, M. Phylogenetic analysis of Bacteroidales 16S rRNA gene sequences from human and animal effluents and assessment of ruminant faecal pollution by real-time PCR. *Journal of Applied Microbiology* **108**, 974–984 (2010).
38. Briand, C. *et al.* Combination of nitrate (N, O) and boron isotopic ratios with microbiological indicators for the determination of nitrate sources in karstic groundwater. *Environ. Chem.* **10**, 365–369 (2013).
39. Zhang, Y., Kelly, W. R., Panno, S. V. & Liu, W.-T. Tracing fecal pollution sources in karst groundwater by Bacteroidales genetic biomarkers, bacterial indicators, and environmental variables. *Science of The Total Environment* **490**, 1082–1090 (2014).
40. Sebiló, M., Mayer, B., Nicolardot, B., Pinay, G. & Mariotti, A. Long-term fate of nitrate fertilizer in agricultural soils. *PNAS* **110**, 18185–18189 (2013).
41. Mariotti, A. *et al.* Experimental determination of nitrogen kinetic isotope fractionation: Some principles; illustration for the denitrification and nitrification processes. *Plant Soil* **62**, 413–430 (1981).
42. Choi, W.-J., Lee, S.-M., Ro, H.-M., Kim, K.-C. & Yoo, S.-H. Natural ^{15}N abundances of maize and soil amended with urea and composted pig manure. *Plant and Soil* **245**, 223–232 (2002).

43. Cravotta, C. A. & Protection, P. D. of E. *Use of stable isotopes of carbon, nitrogen, and sulfur to identify sources of nitrogen in surface waters in the lower Susquehanna River Basin, Pennsylvania*. (U.S. G.P.O., 2002).
44. Rock, L., Ellert, B. H. & Mayer, B. Tracing sources of soil nitrate using the dual isotopic composition of nitrate in 2 M KCl-extracts. *Soil Biology and Biochemistry* **43**, 2397–2405 (2011).
45. Kroopnick, P. & Craig, H. Atmospheric Oxygen: Isotopic Composition and Solubility Fractionation. *Science* **175**, 54–55 (1972).
46. Mayer, B., Bollwerk, S. M., Mansfeldt, T., Hütter, B. & Veizer, J. The oxygen isotope composition of nitrate generated by nitrification in acid forest floors. *Geochimica et Cosmochimica Acta* **65**, 2743–2756 (2001).
47. Liu, T., Wang, F., Michalski, G., Xia, X. & Liu, S. Using ^{15}N , ^{17}O , and ^{18}O To Determine Nitrate Sources in the Yellow River, China. *Environ. Sci. Technol.* **47**, 13412–13421 (2013).
48. Chetelat, B. & Gaillardet, J. Boron Isotopes in the Seine River, France: A Probe of Anthropogenic Contamination. *Environ. Sci. Technol.* **39**, 2486–2493 (2005).
49. Komor, S. C. Boron Contents and Isotopic Compositions of Hog Manure, Selected Fertilizers, and Water in Minnesota. *Journal of Environmental Quality* **26**, 1212–1222 (1997).
50. Millot, R., Petelet-Giraud, E., Guerrot, C. & Négrel, P. Multi-isotopic composition ($\delta^7\text{Li}$ – $\delta^{11}\text{B}$ – δD – $\delta^{18}\text{O}$) of rainwaters in France: Origin and spatio-temporal characterization. *Applied Geochemistry* **25**, 1510–1524 (2010).
51. Briand, C. *Approche multi-traceurs pour la détermination de l'origine de nitrates dans les eaux souterraines: exemple 'une source karstique dans les Landes*. (Pierre et Marie Curie, 2014).
52. McIlvin, M. R. & Altabet, M. A. Chemical Conversion of Nitrate and Nitrite to Nitrous Oxide for Nitrogen and Oxygen Isotopic Analysis in Freshwater and Seawater. *Anal. Chem.* **77**, 5589–5595 (2005).
53. Semaoune, P., Sebilo, M., Templier, J. & Derenne, S. Is there any isotopic fractionation of nitrate associated with diffusion and advection? *Environ. Chem.* **9**, 158–162 (2012).
54. Louvat, P. *et al.* A fully automated direct injection nebulizer (d-DIHEN) for MC-ICP-MS isotope analysis: application to boron isotope ratio measurements. *Journal of Analytical Atomic Spectrometry* **29**, 1698 (2014).
55. Méndez, J. *et al.* Standardised evaluation of the performance of a simple membrane filtration-elution method to concentrate bacteriophages from drinking water. *Journal of Virological Methods* **117**, 19–25 (2004).
56. Ogorzaly, L., Tissier, A., Bertrand, I., Maul, A. & Gantzer, C. Relationship between F-specific RNA phage genogroups, faecal pollution indicators and human adenoviruses in river water. *Water Research* **43**, 1257–1264 (2009).

Acknowledgements

This work was supported by the Water Agency of Adour Garonne and we particularly would like to thank P. Marchet for his great implication in this project. We thank J. Noireaux for her precious help during $\delta^{11}\text{B}$ analyses. MC-ICP-MS was partly funded by the multidisciplinary program PARI of IPGP/region Ile de France (SESAME Grant no. 12015908).

Author Contributions

C.B. wrote the manuscript. C.B., M.Se, V.P., T.C. and P.L. designed the study. C.B., V.V., P.L. and M.Sc performed the analysis. All authors discussed the results and reviewed the manuscript.

Additional Information

Supplementary information accompanies this paper at <http://www.nature.com/srep>

Competing financial interests: The authors declare no competing financial interests.

How to cite this article: Briand, C. *et al.* Legacy of contaminant N sources to the NO_3^- signature in rivers: a combined isotopic ($\delta^{15}\text{N}$ - NO_3^- , $\delta^{18}\text{O}$ - NO_3^- , $\delta^{11}\text{B}$) and microbiological investigation. *Sci. Rep.* **7**, 41703; doi: 10.1038/srep41703 (2017).

Publisher's note: Springer Nature remains neutral with regard to jurisdictional claims in published maps and institutional affiliations.



This work is licensed under a Creative Commons Attribution 4.0 International License. The images or other third party material in this article are included in the article's Creative Commons license, unless indicated otherwise in the credit line; if the material is not included under the Creative Commons license, users will need to obtain permission from the license holder to reproduce the material. To view a copy of this license, visit <http://creativecommons.org/licenses/by/4.0/>

© The Author(s) 2017